J Mater Sci (2007) 42:6426–6432
DOI 10.1007/s10853-006-1188-z

Effect of Y_2O_3 on the crystallization behavior of SiO_2–MgO–B_2O_3–Al_2O_3 glasses

K. Singh · Neha Gupta · O. P. Pandey

Received: 5 March 2006 / Accepted: 30 October 2006 / Published online: 25 April 2007

Abstract A series of glass comprising of SiO_2–MgO–B_2O_3–Y_2O_3–Al_2O_3 in different mole ratio has been synthesized. The crystallization kinetics of these glasses was investigated using various characterization techniques such as differential thermal analysis (DTA), thermo gravimetric analysis (TGA), X-ray diffraction (XRD), and scanning electron microscopy (SEM). Crystallization behavior of these glasses was markedly influenced by the addition of Y_2O_3 instead of Al_2O_3. Addition of Y_2O_3 increases the transition temperature, T_g, crystallization temperature, T_c and stability of the glasses. Also, it suppresses the formation of cordierite phase, which is very prominent and detrimental in MgO-based glasses. The results are discussed on the basis of the structural and chemical role of Y^{3+} and Al^{3+} ions in the present glasses.

Introduction

The planar design of solid oxide fuel cell (SOFC) requires suitable sealant to prevent the fuel gas and air mixing during its operation. It should also provide insulation with proper compatibility to the stack components existing in SOFC. Apart from these it should exhibit chemical stability in reducing and oxidizing atmosphere [1, 2]. Conventional sealing materials do not meet the above-mentioned requirements due to high working temperature (800–1,000 °C) of SOFC and steep change in partial pressure of oxygen (2×10^4–1×10^{-13} Pa) during fuel cell operation.

Suitable composition of glass and glass ceramics meet most of the requirements of an ideal sealant [1, 3, 4]. During the operation of fuel cell, glasses get themselves converted to glass-ceramics and the latter can have different thermal expansion due to crystallization of different phases in glass matrix. Therefore, it is essential to understand the crystallization behavior of glasses under the influence of temperature and time.

In the present study, a series of SiO_2–Al_2O_3–Y_2O_3–MgO–B_2O_3 glasses of different compositions were synthesized. Small amount of B_2O_3 is added to reduce the glass transition temperature, T_g. Al_2O_3 is known to prevent the rapid crystallization of glass during heat treatment, which also prevent the formation of detrimental phase of cristobalite [4, 5]. Y_2O_3 is responsible to increase the thermal expansion coefficient [6]. In the MgO–Al_2O_3–SiO_2 system the formation of different phases take place during crystallization. Among these one of the possible phase is the cordierite ($Mg_2Al_4Si_5O_{18}$) [7]. The cordierite phase however, is detrimental for the SOFC stack since its thermal expansion coefficient (2×10^{-6}/°C) is very low as compared to other components of the fuel cell [3]. The crystallization behavior of the above mentioned glasses were investigated using differential thermal analysis (DTA), thermal gravimetric analysis (TGA), X-ray diffraction (XRD), and scanning electron microscopy (SEM).

Experimental

The selected glass compositions used in the present study with their labeling as GS1, GS2, GS3, GS4 are given in

K. Singh (✉) · N. Gupta · O. P. Pandey
School of Physics and Materials Science, Thapar Institute of Engineering and Technology (Deemed University), Patiala 147004, Punjab, India
e-mail: ksbadla@yahoo.co.in

Table 1 Sample label with constituents in mol.%

Sample label	SiO_2	Al_2O_3	Y_2O_3	MgO	B_2O_3
GS1	45	10	0	40	5
GS2	45	8	2	40	5
GS3	45	6	4	40	5
GS4	45	4	6	40	5

Table 1. The glasses were prepared by taking stoichiometric amounts of different constituents in the form of oxides and carbonates (purity ≥ 99.5%). For each batch appropriate mole fraction of initial ingredients were mixed under the wet media (acetone) using mortar and pestle for 2 h. The mixed powders of these samples were first dried in oven at 150 °C and melted in alumina crucible at 1,550 °C. The melt was held at this temperature for half an hour to ensure homogenization. After this crucible was removed from furnace and the melt was poured on the flat copper plate and quenched by other copper plate in air to obtain thick flakes. The as prepared glasses were characterized by X-ray diffraction (XRD; D/Max Rint 2000 Rigaku, Tokya) for the confirmation of glassy nature as well as to find out the crystalline phases after heat treatment at 1,000 °C for 1, 9 and 100 h time duration. The glass transition temperature (T_g) and crystallization temperature (T_c) were determined by DTA. The DTA analysis was performed in air on powdered samples at the heating rate of 10 °C/min [Perkin Elmer, USA]. The glass stability and weight loss was checked by a TGA (Mettler) in the range of room temperature to 1,200 °C at a heating rate of 10 °C/min in N_2 atmosphere. Microstructural studies were carried out using SEM (Joel, JSM-840A) on heat-treated sample of GS4 glass at 1,000 °C for 1, 9 and 100 h. For structural analysis, glass pieces taken from different areas of sample after heat treatment were mounted in a cylindrical mold using acrylic powder and liquid. These mounted samples were mechanically polished. The final polishing was done on 0.25 μm diamond grit. In order to ensure smoothness of the sample surface, the samples were examined under optical microscope before etching. The samples were finally etched with 20% hydroperchloric acid to reveal structure. For SEM studies gold sputtering was done on the surface of samples to make the surface conducting.

Results and discussion

The as prepared glasses of all the above four compositions were found to be amorphous in nature as all of them exhibited a broad peak in the X-ray diffraction pattern. A typical XRD of GS4 sample is shown in Fig. 1. These glass samples were further subjected to heat treatment at

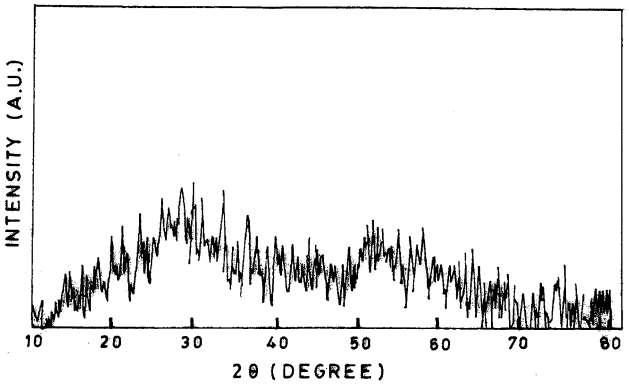

Fig. 1 XRD pattern of as prepared glass sample GS4 showing the amorphous nature of the glass

1,000 °C for 1, 9 and 100 h time duration to understand the nucleation kinetics of different phases with aging time at elevated temperature. The X-ray diffraction patterns of all the heat-treated glasses exhibit the formation of various crystalline phases that were identified using powder diffraction files (PDF). All the glass ceramics, where Y_2O_3 was added at the cost of Al_2O_3 exhibit only the formation of $MgSiO_3$ and Mg_2SiO_4 phases after heat treatment. However, apart from these phases the sample GS1 additionally exhibited $Mg_{0.6}Al_{1.2}Si_{1.8}O_6$ solid solution phase [PDF file no. 75-1568]. The volume fraction of this $Mg_{0.6}Al_{1.2}Si_{1.8}O_6$ phase in GS1 was observed to increase with increasing heat treatment duration at the cost of $MgSiO_3$ phase as is evident in Fig. 2. This means that aging time leads to growth of $Mg_{0.6}Al_{1.2}Si_{1.8}O_6$ phase and a decrease in $MgSiO_3$ phase. According to Zdaniewski [8] in MgO–SiO_2 based glasses, the early stage of crystallization occurs by formation of a SiO_2 rich solid solution phase and subsequently in the latter stage an isomorphic substitution of Mg^{2+} and Al^{3+} occurs at different sites of the unit cell. This substitution takes place in such a way that the composition approaches to that of $Mg_{0.6}Al_{1.2}Si_{1.8}O_6$ phase apart from formation of $MgSiO_3$ and Mg_2SiO_4 phases. The XRD pattern of this particular sample shows the shifting in XRD lines at lower angles with increasing heat treatment duration indicating a change in lattice parameter (Fig. 2). This might be attributed to $Mg_{0.6}Al_{1.2}Si_{1.8}O_6$ phase that is not a pure one but a solid solution phase. Initially this phase nucleates as Si rich phase and at latter stages of the heat treatment Al^{3+} ions occupy Si^{4+} ion sites. Since Al^{3+} ions are larger than Si^{4+} ions it would be responsible for the enhancement in lattice parameter of $Mg_{0.6}Al_{1.2}Si_{1.8}O_6$ phase. However, the peak shifting could not be observed in case of $MgSiO_3$ and Mg_2SiO_4 phases except variation in relative peak intensity. This can be understood from the following chemical reactions:

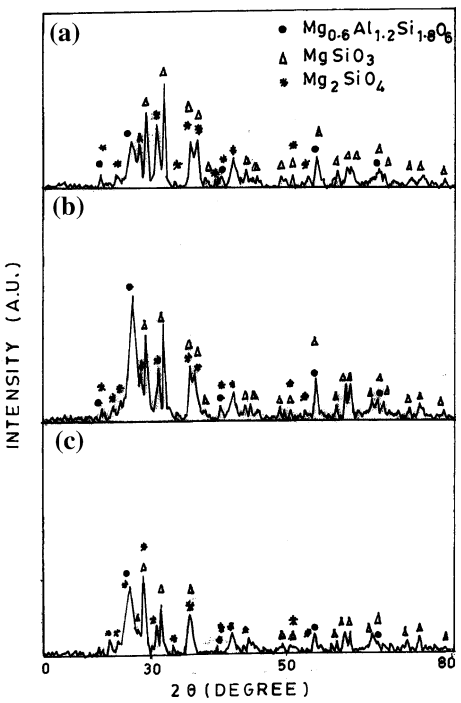

Fig. 2 XRD pattern of glass sample GS1 after (**a**) 1 h heat treatment, (**b**) 9 h heat treatment and (**c**) 100 h heat treatment at 1,000 °C showing the presence of different crystalline phases

$$3MgO + 2SiO_2 \rightarrow MgSiO_3 + Mg_2SiO_4 \qquad \text{(I stage)}$$

$$3MgSiO_3 + 3SiO_2 + 2Al_2O_3 \rightarrow MgSiO_3 + Mg_2Al_4Si_5O_{18} \qquad \text{(II stage)}$$

It is obvious from above reaction that in the beginning the nucleation of solid solution silicon rich phase takes place and at the latter stage the migration of ions takes place and composition shifts to $Mg_2Al_4Si_5O_{18}$. On the other hand, glasses containing Y_2O_3 do not exhibit the cordierite phase. A typical X-ray diffractogram for all the glasses studied (GS1, GS2, GS3, GS4) and which were heat treated at 1,000 °C for 9 h are shown in Fig. 3**.** Since, thermodynamically Mg_2SiO_4 phase is more stable as compared to $MgSiO_3$, the volume fraction of Mg_2SiO_4 phase keeps on increasing at the expense of $MgSiO_3$ phase in all these samples as is evident in Fig. 3. The suppression of cordierite phase in GS2, GS3 and GS4 samples could be explained on the basis of the presence of extra cation like yttria which increases the competition among other cations which may prevent the formation $Mg_{0.6}Al_{1.2}Si_{1.8}O_6$ phase and excess amount of crystallization [9]. However, the field strength of Y^{3+} ion is less as compared to Al^{3+} ions in glass compositions as shown in Table 2.

The TGA spectra of all four-glass samples (GS1, GS2, GS3, GS4) are given in Fig. 4. Addition of Y_2O_3 significantly increases the stability of the samples. In GS2 sample, addition of 2% Y_2O_3 at the cost of Al_2O_3 significantly decreases the percent weight loss relatively to sample GS1. A further increase in Y_2O_3 content in samples was found to improve the stability of the samples. In the subsequent samples, addition of Y_2O_3 stabilizes, the glasses and thereby decreases in the weight loss as indicated in Table 3. This might be because of the less crystallization of Y_2O_3 rich glasses as compared to GS1 sample during heat treatment. The above consideration is also supported by the fact that the width of XRD peaks, which increase with increasing Y_2O_3 contents as can be seen from Fig. 3.

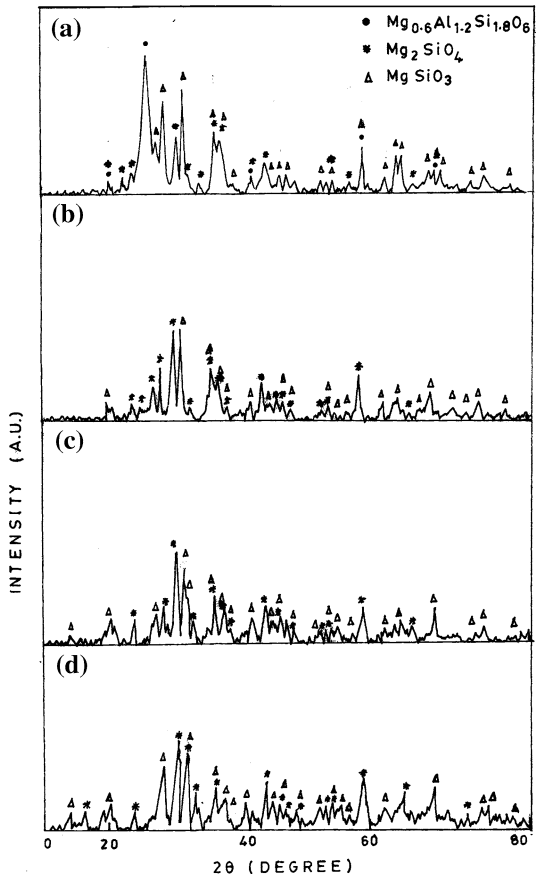

Fig. 3 XRD pattern of glass samples (**a**) GS1, (**b**) GS2, (**c**) GS3 and (**d**) GS4 after 9 h heat treatment at 1,000 °C showing the variation in peak intensities of different phases

Table 2 Field strength of Y, Si, Al, B and Mg cations

Elements	Valency	Ionic radius (A_o)	Ionic distance $(r_c + r_a)A_o$	Field strength $[Z + /(r_c + r_a)^2]$
Si	4	0.39	1.71	1.37
Y	3	1.06	2.38	0.53
Al	3	0.57	1.89	0.84
B	3	0.20	1.52	1.29
Mg	2	0.78	0.78	0.45

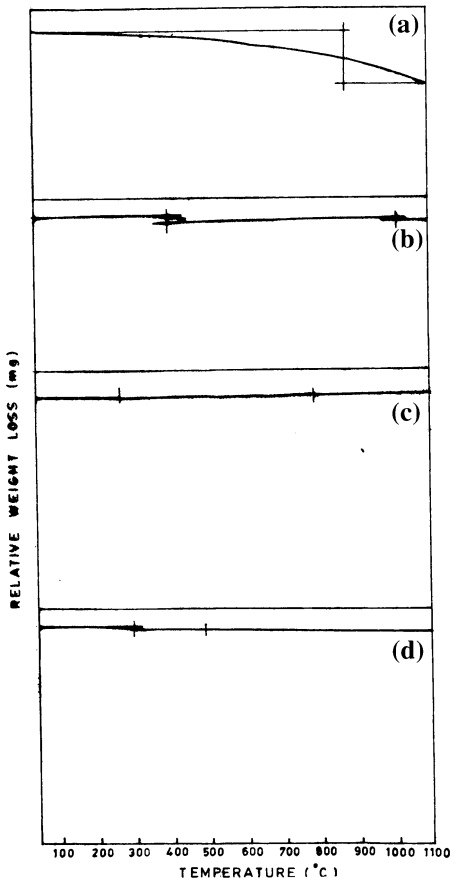

Fig. 4 TGA spectra of (**a**) GS1, (**b**) GS2, (**c**) GS3 and (**d**) GS4 samples showing the mass loss characteristics of these glass samples

Table 3 Glass transition temperature T_g, crystallization temperature T_c, % weight in loss of the investigated glasses

Label	T_g (°C)	T_c (°C)	% Change in weight
GS1	670	865	4.8
GS2	700	905	2.0
GS3	704	945	0.07
GS4	727	995	0.6

In order to check the glass transition and crystallization temperature, the DTA was performed on these glasses with the heating rate of 10 °C/min. A typical DTA curve for GS2 and GS4 are given in Fig. 5a, b. Besides the glass transition temperature, all the samples exhibit an exothermic peak. However, this exothermic peak is very weak in GS1 sample. Apart from T_g and exothermic peak, the GS3 sample also showed a weak endothermic peak. In general, SiO_2–MgO–Al_2O_3 glasses undergo phase separation when Al_2O_3 content is more than 5 mol.% in the glass composition [10, 11]. Phase separation in these glasses occurs when a metal cation other than Si^{4+} has a certain degree of

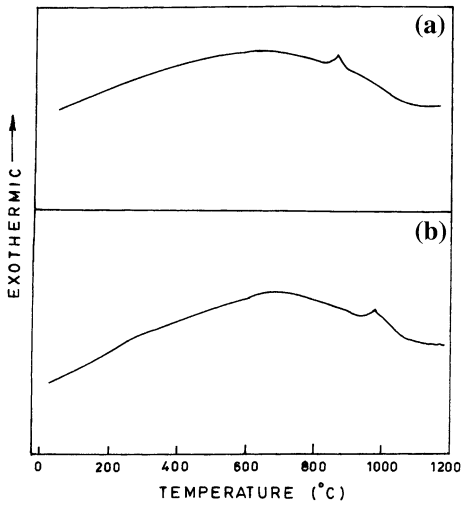

Fig. 5 DTA spectra of (**a**) GS2, and (**b**) GS4 samples showing the exothermic peaks

ionic field strength as indicated in Table 2. However, it is established fact that if there are several kinds of cations having field strength high enough to attract oxygen ions then phase separation does not occur due to competition between the cations themselves [12]. But, in present case, the phase separation could not be observed even the content of Al_2O_3 is more than 5 mol.% as reported in earlier studies on the similar systems [8]. The tendency of Al_2O_3 to induce phase separation depends upon the occupancy of Al^{3+} cations in different interstitial sites. There can be four or six coordination numbers of Al^{3+} cation with oxygen giving rise to either tetrahedral AlO_4 or octahedral AlO_6. When it is tetrahedrally coordinated, it takes part as network former. But at the same time, when the coordination number changes to six, it works as network modifier [3]. Basically, the presence of cations of single and double valence state such as Mg^{2+} is known as network modifier cations. A modifier induces such changes by breaking some fraction of the Si–O bonds thereby creating no bridging oxygen and disturbing the tetrahedral silicate network. The non-bridging oxygen (NBO) provides relatively weak connections between the network forming atoms and the network modifier cations. However, when other network forming ions such as Al^{3+} and Y^{3+} are introduced into the system, there is gradual conversion of NBO to bridging oxygen (BO). In the present case, the Al^{3+} ions may be tetrahedral coordinated so second exothermic peak could not be observed in these samples. This indicates that phase separation not only depend on Al_2O_3 content but also on processing conditions of the samples. It is very interesting to note that the addition of Y_2O_3 in starting material increases T_g and T_c with decreasing ratio of Al_2O_3/Y_2O_3. This might be attributed due to Y^{3+} cation that is coordinating

tetrahedrally and it acts as a glass former. Apart from this, a decrease in Al_2O_3 content from GS1 to GS4 is also responsible to an increase in T_g and T_c in all the glass samples studied. Yttrium being larger size metal offers higher coordination number [13] so it can act as network former. However, the field strength of Y^{3+} ion is less than Al^{3+} ion. Lahl et al. [5] suggested that when TiO_2, Cr_2O_3 and Ni are added in MgO based aluminosilicate glasses, it enhances the activation energy of these systems whereas ZrO_2 decreases activation energy. The reason for this is because of high field strength of hexavalent Zr^{2+} and Ti^{4+} which leads to ordering characteristic in these glasses.

In order to understand the properties of these glasses during long time exposure at high temperature it is essential to understand the variation in microstructure of these samples during heat treatment. Out of all glasses, GS4 showed good stability in TGA analysis so a detail SEM study was carried out for this sample.

Figure 6a–f shows the SEM micrographs of the GS4 sample after 1 (a and b), 9 (c and d) and 100 (e and f) hours of heat treatment. The important feature in all these micrographs are the uniformly distributed needle like precipitate, which can be seen throughout the structure. The flow pattern existing in all the samples, which is more pronounced at higher magnification, indicates that the undercooled glass has developed more stresses during quenching process. These areas have provided site for the nucleation of crystalline phases in the glass matrix. In general all the samples, which were heat-treated, exhibit the simultaneous growth of the two different phases during heat treatment, which is evident in all the micrographs taken from different areas of the samples.

Figure 6a, b is SEM micrograph of GS4 sample aged at 1,000 °C for 1 h. It is evident from the micrograph that two types of phases appear during heat treatment one fine long needle type of structure and other coarser blunt needle. The low magnified micrograph (Fig 6a) reveals the uniform distribution of crystalline needle like phases in the glass matrix. In the higher magnification micrograph (Fig. 6b) these needle like structure is more clear. These crystalline phases are Mg-rich, which were confirmed through electron probe micro-analysis (EPMA). Figure 7 is a typical EDAX spectrum taken from these areas. It shows the presence of Mg, Si and Ca elements. Our atomic absorption spectrometer (AAS) analysis revealed that Ca is present in traces (0.02188 wt.%). The analysis was done on five

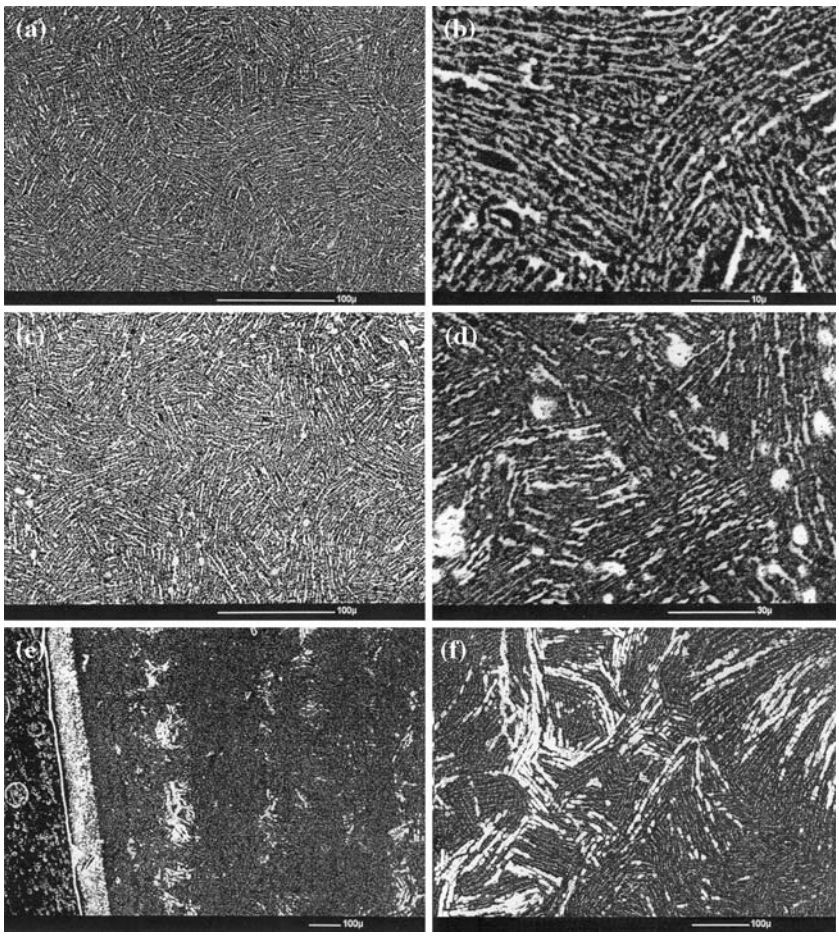

Fig. 6 SEM micrograph of GS4 sample (**a**, **b**) after 1 h heat treatment (**c**, **d**) after 9 h heat treatment and (**e**, **f**) after 100 h heat treatment at 1,000 °C showing the transformation characteristics of crystalline phases

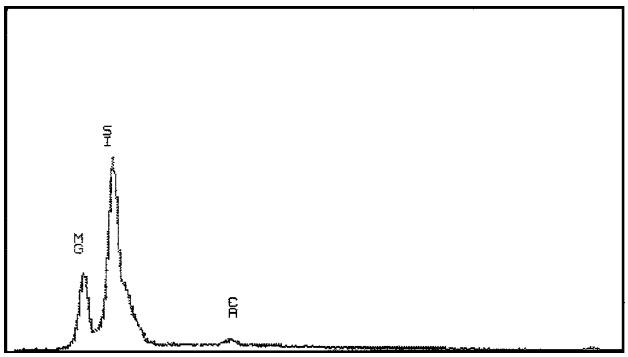

Fig. 7 EDAX spectrum of GS4 glass showing the presence of elements in it

samples in which results varied from 0.02438 to 0.01870 wt.%. The presence of Ca in traces is because of impurity in the raw material taken for preparation of glasses. During course of melting it may get segregated to form calcium silicate phase. Since such types of phases are not present in our X-ray analysis so existence of such peak does not carry any meaning. Initially $MgSiO_3$ phase nucleates as fine needle like structure. During ageing, this finely nucleated structure starts collapsing and turn out as bigger structure. The structure appears to be a composite type where crystalline phases, one comprising of $MgSiO_3$ and another Mg_2SiO_4 which are embedded in glass matrix. As the ageing time proceeds the volume fraction of Mg_2SiO_4 phase increases. Figure 6c, d is the micrograph of the GS4 sample aged for 9 h where one can see the transition of $MgSiO_3$ phase into Mg_2SiO_4 phase. EPMA showed higher concentration of Mg at coarser blunt needle as compared to fine long needles. Since the X-ray analysis confirmed the presence of $MgSiO_3$ and Mg_2SiO_4 phases, it is obvious that fine needle like structure comprising of lesser amount of Mg represent for $MgSiO_3$ phase and coarse blunt bright phase containing higher amount of Mg represent Mg_2SiO_4 phase (Fig. 6d). The process of this growth is similar to that of well-known Ostwald-ripening phenomenon [14].

In order to understand the growth of one phase at the expense of another with passage of time at same heat treatment temperature in detail, the samples taken from different areas of GS4 glass were further given heat-treatment at 1,000 °C for 100 h. Figure 6e, f is a typical micrograph of such sample. The low magnification micrograph reveals the banded morphology [15–17], which exists at the edges as well as at the center of the sample. The micrograph further supports our view that growth of Mg_2SiO_4 phase occurs as the conditions (time and temperature) becomes more favorable for it. A higher magnification micrograph taken from brighter area (Fig. 6f) reveals the morphological feature of Mg_2SiO_4 phase that get itself rearranged. The existence of more pronounced banded structure (Fig. 6e) indicates that the volume fraction of the second phase (Mg_2SiO_4) appears to be more as time duration of heat treatment increases. The nucleation and growth of the typical structure all along the edges of the sample with a fine band is an indication of the fact that second phase has nucleated from the defect sites where stress concentration is more. On comparing the structure of samples heat treated for 9 h taken from different areas (central and edges), it can be concluded that the formation and growth of Mg_2SiO_4 phase is more rapid at the edges (Fig. 6d) as compared to the central zone (Fig. 6c). This is because of the fact that this growth phenomenon is more sluggish as both the phases belongs to the same family and is dependent on temperature and aging time. Since, the surface experiences the fluctuation in temperature more rapidly as compared to inner core because of ''on'' and ''off'' conditions of the furnace during heat treatment at the desired temperature, it develops more thermal stresses. As the condition prevails for longer duration the nucleation of $MgSiO_3$ takes place heterogeneously at these stress concentration points which further transforms to Mg_2SiO_4 as thermodynamically it is more stable phase. This is the reason that volume fraction of Mg_2SiO_4 phase is more at the edges as compared to center of the specimen. However, in order to understand this growth and the resultant morphology it is essential to go for longer aging time beyond 100 h.

As described above an important feature observed in the sample GS4 heat-treated for 9 and 100 h is those two types of structural features one corresponding to very fine (needle like) and another one (blunt type) of a structure (Fig. 6d). The coherent matching between these two phases and the flow pattern observed indicates that the earlier nucleated $MgSiO_3$ phase is being transformed to another phase Mg_2SiO_4 of the same family having the same crystallographic directions of their growth.

A study carried out using differential drop solution calorimetric technique indicate that $MgSiO_3$ (ilmenite) transform to $MgSiO_3$ (pervoskite) structure and similarly Mg_2SiO_4 (spinel) also transforms to $MgSiO_3$ (perovskite) structure [18]. The ilmenite–pervoskite transition in $MgSiO_3$ is associated with 110.1 ± 4.3 kJ/mole for the enthalpy. In an another study on MgO–SiO_2 system on interatomic potential model developed using columbic term, a born repulsive term and a Vander Walls term for oxygen–oxygen interaction indicate the transformation of $MgSiO_3$ (ilmenite) to $MgSiO_3$ (perovskite) and Mg_2SiO_4. The feasibility of transformation is because of variation in coordination number of Si (octahedral and tetrahedral) [19]. Since $MgSiO_3$ [20] and Mg_2SiO_4 [21] exhibit same crystal structure with variation in lattice parameter though their nature of bonding varies as coordination number also

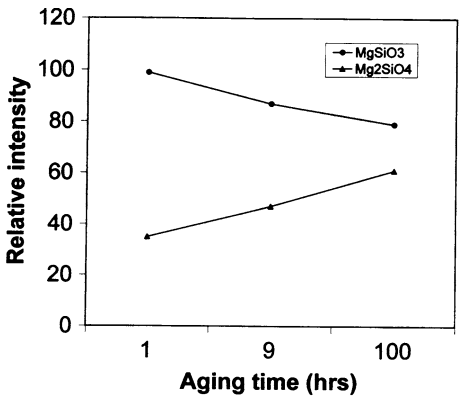

Fig. 8 Variation of relative intensity with aging time in X-ray diffractrogram for $MgSiO_3$ and Mg_2SiO_4 phases present in GS4 sample when heat-treated at 1,000 °C

varies, it is possible that $MgSiO_3$ phase can transform to Mg_2SiO_4 phase under the influence of thermal and concentration gradient. Our X-ray analysis revealed the presence of solid solution phase, $MgSiO_3$ and Mg_2SiO_4 phases. Also the volume fraction of Mg_2SiO_4 phase is increasing with increase in heat treatment time. The EPMA analysis also revealed that blunt type needles are of Mg-rich phase. Based on above studies followed by support from literature it can be said that the transformation of $MgSiO_3$ phase to Mg_2SiO_4 phase occurs as the heat treatment duration is increased. Because of the fact that both exhibit orthorhombic crystal structure with variation in lattice parameter, they will have the same crystallographic growth direction.

The X-ray analysis indicates that the sample GS4 which has been given heat treatment for 1 h at 1,000 °C contains higher volume fraction (relative intensity 99%) of $MgSiO_3$ phase. On subsequent increment in ageing time leads to a decrease in the relative intensity of $MgSiO_3$ phase and an increase in Mg_2SiO_4 phase (35–61%) as the aging time is increased from 1 to 100 h as shown in Fig. 8. The microstructural features observed and the X-ray analysis done for the glasses indicates that Mg_2SiO_4 phase is more stable as compared to $MgSiO_3$ (Fig. 8). Since these two phases belongs to same category, the growth of thermodynamically stable Mg_2SiO_4 phase with increasing ageing time on the expense of $MgSiO_3$ phase is obvious.

Conclusion

SiO_2–Al_2O_3–Y_2O_3–MgO–B_2O_3 glasses made were initially amorphous which subsequently transferred into crystalline phases with the formation of $MgSiO_3$ and Mg_2SiO_4 phases. Apart from these phases, sample GS1 also exhibit the presence of cordierite phase, which is detrimental for SOFC. The volume fraction of the cordierite phase increases with increase in the heat treatment time in the glass sample GS1.

The addition of Y_2O_3 completely suppresses the formation of cordierite phase in the rest of the glasses. Also, it enhances the stability of the glasses. The volume fraction of Mg_2SiO_4 phase was observed to increase with increasing heat treatment time. The SEM and XRD studies clearly indicate that Mg_2SiO_4 phase grows on the expense of $MgSiO_3$ phase, which is a stable one. The stability of the samples increases with the addition of Y_2O_3. The crystallization and glass transition temperature is also found to increase with the increase in yttrium content.

Acknowledgement For carrying out this research the financial assistance provided by All India Council for Technical Education (AICTE), New Delhi and Department of Science and Technology (DST) is highly acknowledged.

References

1. Ley KL, Krumpel M, Meisser TR, Bloom I (1996) J Mat Res 11:1449
2. Eichler K, Solow G, Otschil P, Schaffrath W (1999) J Eur Ceram Soc 19:1101
3. Sung YM (1996) J Mater Sci 31:5421. DOI: 10.1007/BF01159312
4. Lahl N, Singh K, Singheiser L, Hilpert K, Bahadur D (2000) J Mater Sci 35:3089. DOI: 10.1023/A: 1004851418274
5. Lahl N, Bahadur D, Singh K, Singheiser L, Hilpert K (2002) J Electrochem Soc 149:A607
6. Schwickert T, Sievering R, Geasee P, Conradt R (2002) Mattwisu Werkstofftech 33:363
7. Lara C, Pauscal MJ, Duran A (2004) J Non-Cryst Solids 348:149
8. Zdaniewski W (1975) J Am Ceram Soc 58:163
9. Yun-Mo-Sung (2002) J Mater Res 17:517
10. Mac Dowell JF, Beall GH (1969) J Am Ceram Soc 52:17
11. Davis RF, Pask JA (1972) J Am Ceram Soc 55:525
12. Bahadur D, Lahl N, Singh K, Singheiser L, Hilpert K (2004) J Electrochem Soc 15:A558
13. Lee JD (1993) Concise inorganic chemistry, 4th edn. Chapman and Hall, London, p 683
14. Madras G, Coy BJ (2001) J Chem Phys 115:6699
15. Zimmermann M, Carrard M, Kurz W (1989) Acta Metall 37:3305
16. Zimmermann M, Carrard M, Gremand M, Kurz W (1995) Mat Sci Eng A 134:1278
17. Grimand M, Carrard M, Kurz W (1990) Acta Metall Mater 38:2587
18. Ito E, Akaogi M, Topor L, Navrotsky A (1990) Science 249:1275
19. Leinenweber K, Navrotsky A (1988) Phys Chem Minerals 15:588
20. Yagi T, Mao HK, Bell PM (1978) Phys Chem Minerals 3:97
21. Horiuchi H, Sawamoto H (1981) Am Mineral 66:568